X. Jack Hu[1]
e-mail: jack.hu@intel.com

Antonio A. Padilla

Mechanical Engineering Department,
Stanford Univeristy,
440 Escondido Mall,
Stanford, CA 94305

Jun Xu

Timothy S. Fisher

School of Mechanical Engineering and Birck
Nanotechnology Center,
Purdue University,
585 Purdue Mall,
West Lafayette, IN 47907

Kenneth E. Goodson
Mechanical Engineering Department,
Stanford University,
440 Escondido Mall,
Stanford, CA 94305

3-Omega Measurements of Vertically Oriented Carbon Nanotubes on Silicon

An exploratory thermal interface structure, made of vertically oriented carbon nanotubes directly grown on a silicon substrate, has been thermally characterized using a 3-omega method. The effective thermal conductivities of the carbon nanotubes (CNT) sample, including the effects of voids, are found to be 74 W/m K *to* 83 W/m K *in the temperature range of* 295 K *to* 323 K*, one order higher than that of the best thermal greases or phase change materials. This result suggests that the vertically oriented CNTs potentially can be a promising next-generation thermal interface solution. However, fairly large thermal resistances were observed at the interfaces between the CNT samples and the experimental contact. Minimizing these contact resistances is critical for the application of these materials.* [DOI: 10.1115/1.2352778]

Keywords: thermal conductivity, contact thermal resistance, carbon nanotube, thermal interface material, 3-omega method, thermal management

Introduction

Excessive chip heating is becoming a major cause of failures in electronic components and a critical obstacle in developing more advanced electronic devices. Related to this problem is the fact that the thermal interface materials (TIMs), used for attaching an electronic chip to its heat spreader or heat sink, have very low thermal conductivity, which causes large thermal resistances at packaging interfaces. These interface resistances are in series with the resistance of any heat sink and cannot be removed or reduced by using advanced cooling techniques on the heat sink side. Because chip sizes are remaining the same and power dissipation continues to increase, without improvements in TIM thermal conductivity, the temperature rise at package interfaces will increase proportionally and occupy an increasing fraction of the total allowable junction-to-ambient temperature rise. According to the projection of the International Technology Roadmap for Semiconductors [1], by the year of 2010, if TIM thermal conductivity remains the same, the overall thermal resistance budget will be completely occupied by the TIM resistance, and performance improvements in electronic chips may no longer be sustained. To meet the increasing power dissipation requirements, large improvements in TIM thermal conductivity are needed in next few years.

Carbon nanotubes (CNTs), a man-made material first reported by Iijima in 1991 [2], are promising candidates for improving TIM thermal conductivity. Many reports suggest CNTs to be the best heat conductor among all the materials. Hone et al. [3] found that the thermal conductivity of aligned single-wall nanotube (SWNT) ropes is about 250 W/m K at 300 K and estimated that the thermal conductivity of a single SWNT in the longitude direction ranges from 1750 W/m K to 5800 W/m K. The thermal conductivity of individual CNTs (multiwall nanotube (MWNT) [4] or SWNT [5]) has been measured to be at least 3000 W/m K at room temperature, which is about eight times higher than that of copper and 20 times higher than that of silicon. Theoretical studies predict even higher thermal conductivity values, such as 6600 W/m K at room temperature by Berber et al. [6].

Owing to their high thermal conductivity, CNTs have received much attention for thermal management in recent years. Early attempts used CNTs as fillers to form high thermal conductivity fluids or TIM composites. Choi et al. [7] measured the effective thermal conductivity of nanotube-in-oil suspensions and found that with only 1 vol % of nanotubes, the effective thermal conductivity can be 2.5 times the value of the base fluid. Such an increase in thermal conductivity has never been found previously with any other particles. Biercuk et al. [8] also found that epoxy filled with 1 wt % of CNTs exhibited a 70% increase in thermal conductivity at 40 K and 125% at room temperature. Hu et al. [9] proposed the combined use of CNTs and traditional heat conductive fillers for TIMs. They achieved a thermal conductivity value seven times that of the base material, almost double the thermal conductivity of the corresponding TIM composite with only traditional fillers. However, this thermal conductivity value is still one thousandth that of an individual CNT. The potential heat conduction capability of CNTs is far from optimal.

Two problems can lead to the low efficiency. One problem is that CNTs are randomly dispersed, and only a few portions of CNTs are effectively contributing to heat conduction. The other problem is that heat is not directly conducted from one side to the other through CNTs. CNTs are discontinued by other fillers or the base fluid. The low thermal conductivity of the interstitial media, as well as the contact resistance between those and CNTs, degrades the thermal performance of the CNT composites.

A more advanced approach is to grow CNTs directly on a sili-

[1]Current address: Intel Corporation, 5000 W Chandler Blvd, CH5-157, Chandler, AZ 85226.

Contributed by the Heat Transfer Division of ASME for publication in the JOURNAL OF HEAT TRANSFER. Manuscript received February 24, 2005; final manuscript received November 4, 2005. Review conducted by Yogendra Joshi. Paper presented at the 2005, IEEE Semiconductor Thermal Measurement, Modeling, and Management Symposium.

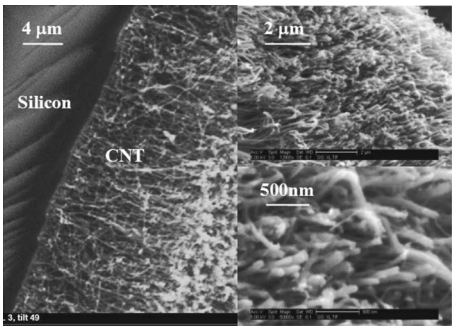

Fig. 1 SEM images of the CNT sample

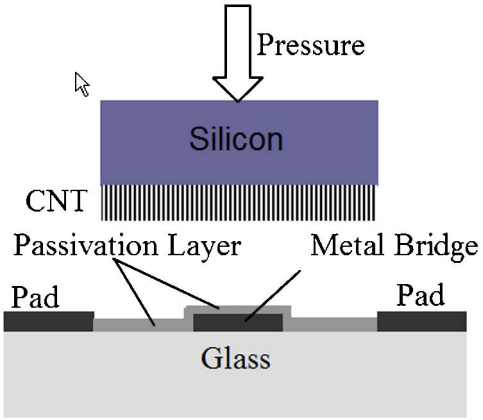

Fig. 2 Schematic of the experimental structure

con wafer and oriented CNTs in the direction of heat conduction (i.e., perpendicular to the silicon wafer). These CNTs can be attached to a copper heat spreader and serve as a thermal interface structure [10]. Xu and Fisher [11] first tested such a structure using a 1D steady-state method. This test, however, can only yield a total thermal resistance, summed over the depth of the CNT layer including interfaces, and suffered from relatively large uncertainties. In this paper, we develop an MEMS-based frequency-domain measurement to precisely characterize the thermal properties of the aligned CNT sample and contact resistances. Various challenges in using the aligned CNTs as an interfacial structure and possible solutions are also discussed.

Experimental Measurements

Sample Preparation. The CNT samples are grown on 7 mm $\times$7 mm double-side-polished silicon chips using direct synthesis with a trilayer (Ti-Al-Ni) catalyst configuration and microwave plasma enhanced chemical vapor deposition (PECVD) (the same process as [11]). The thicknesses of the titanium, aluminum, and nickel layers are 30, 10, and 6 nm respectively, and the thickness of the silicon substrate is about 420 μm. The H_2/CH_4 plasma is excited at a chamber pressure of 10 Torr and a microwave power of 150 W. The synthesis temperature is maintained at 800°C.

Figure 1 shows scanning electron microscope (SEM) images of the synthesized CNTs on a silicon substrate. Vertically oriented, multiwalled CNTs evenly cover all over the silicon substrate. The length of the CNT layer is about 13 μm, and the diameters range from 10 nm to 80 nm. The two images on the right side are taken after the measurements, suggesting that the CNT sample can withstand an attachment pressure up to 100 kPa without noticeable degrading in quality.

Measurement Method. A schematic of the experimental structure is given in Fig. 2. The CNT sample, with the CNT-side facing downward, is attached to a test device under a controlled attachment pressure. The test device is fabricated on a glass wafer to reduce heat loss from the substrate and contains a microscale patterned metal bridge operated in the kilohertz regime using the 3ω technique (for reviews of the 3ω technique see [12,13]). The metal bridge is a platinum line, 7 mm long, 50 μm wide, and 200 nm thick, with four-wire electrical connects. Beneath the metal bridge, a 0.5 nm titanium layer is used to ensure good adhesion to the substrate; and on top of the metal bridge, 20 nm silicon nitride is deposited to insulate the electrical conductive bridge from the CNT sample.

The experimental structure, attached with a chip carrier, is placed in a Lakeshore MTD-135 cryostat chamber and connected in an electrical circuit as shown in Fig. 3. The metal bridge serves both as a heater and a thermometer. Driven by the sine out of a SR830 lock-in amplifier at an angular frequency of ω, the metal bridge generates joule heat and produces a temperature oscillation ΔT at 2ω. It is noted that the electrical resistance of the metal bridge is proportional to its temperature, and thus the electrical resistance is also modulated at 2ω. With the applied current at ω, the voltage drop along the metal bridge thus contains a modulated component at 3ω. This 3ω voltage component, $V_{3\omega}$ is related to the temperature oscillation ΔT as [12]

$$\Delta T = 2\frac{dT}{dR}\frac{R_0}{V}V_{3\omega} \tag{1}$$

where V is the applied voltage and R_0 is the electrical resistance along the metal bridge, respectively, and dT/dR depicts the temperature dependence of R_0, which is calibrated at chamber temperatures ranging from 295 K to 324 K. After subtracting the ω voltage component using a Wheatstone bridge, as shown in Fig. 3, $V_{3\omega}$ is determined by measuring the nonequilibrium voltage $v_{3\omega}$, using the SR830 lock-in amplifier. The conversion from $v_{3\omega}$ to $V_{3\omega}$ is given by [14]

$$V_{3w} = \frac{(R_0 + R_1)\cdot(R_2 + R_3)}{R_1\cdot(R_2 + R_3)}v_{3w} \tag{2}$$

Thermal Model and Data Analysis. We model the transient heat conduction problem using a one-dimensional (1D) model. 1D heat conduction is a good approximation because the width of the heater is several times larger than the thickness of the CNT layer (50 μm versus 13 μm), and more importantly, because the thermal coupling between CNTs is weak and the in-plane heat conduction in the CNT layer is negligible. If not specially noted, the thermal conductivity of the CNT layer in this paper is always considered in the longitude direction.

For 1D heat conduction in a homogeneous medium, if only the

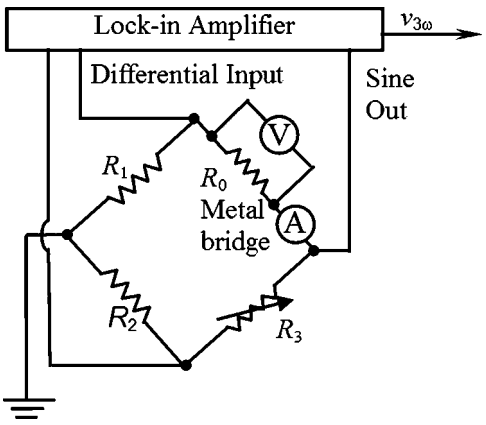

Fig. 3 Electronic circuit of the experimental system [14]

temperature difference relative to its substrate is considered, the periodic steady-state heat conduction equation in the frequency domain can be written as

$$\frac{d^2\Delta T(x,\omega)}{dx^2} = a^2\Delta T(x,\omega) \tag{3}$$

with boundary conditions

$$-k\frac{d\Delta T(x,\omega)}{dx}\bigg|_{x=0} = P'' \tag{4}$$

$$\Delta T(l,\omega) = 0 \tag{5}$$

where $a=\sqrt{j\omega\rho c/k}$, j is imaginary unit, ρ, c, k, l are the density, specific heat, thermal conductivity, and thickness of the media, P'' is the applied power density, and ω is the angular frequency of the heat flux. The solution of this differential equation at $x=0$ and a given frequency ω is

$$\Delta T(\omega) = \frac{P''\tanh(al)}{ak} \tag{6}$$

If we define a thermal impedance as $Z(\omega)=\Delta T(\omega)/P''$, then

$$Z(\omega) = \frac{\tanh(al)}{ak} \tag{7}$$

For small al, $\tanh(al)\approx 2al/(2+a^2l^2)$ by neglecting $O(a^3L^3)$ terms, resulting in

$$Z^{-1}(\omega) = R^{-1} + j\omega C \tag{8}$$

with thermal resistance

$$R = l/k \tag{9}$$

and thermal capacitance

$$C = \rho cl/2 \tag{10}$$

As $al\to\infty$, $\tanh(al)\to 1$, and

$$Z^{-1}(\omega) = \sqrt{j\omega\rho ck} = \sqrt{\omega\rho ck/2} + j\omega\sqrt{\rho ck/(2\omega)} \tag{11}$$

The thermal resistance and thermal capacitance for a semi-infinite medium thus can be expressed as

$$R = \sqrt{2/(\omega\rho ck)} \tag{12}$$

and

$$C = \sqrt{\rho ck/(2\omega)} \tag{13}$$

The layer of CNT can be modeled as a thin film by introducing an effective thermal conductivity

$$k_{e,CNT} = \phi k_{CNT} + (1-\phi)k_{air} \approx \phi k_{e,CNT} \tag{14}$$

and effective volume-based specific heat

$$C_{e,CNT} = \phi(\rho c)_{CNT} + (1-\phi)(\rho c)_{air} \tag{15}$$

The two substrates (silicon and glass) are modeled as semi-infinite media, and the corresponding thermal resistance and thermal capacitance are given by Eqs. (12) and (13). Between the CNT sample and the heater, a contact thermal resistance R_c exists, which can be caused by the impacts of imperfect contact, boundary scattering as well as passivation and catalyst. No capacitance term exists at the contacts because the passivation and catalyst layers are extremely thin (<0.07 μm in total), without contribution to heat storage.

Thus the transient heat conduction problem can be modeled using the equivalent thermal circuit given in Fig. 4. It should be noted that the CNT capacitor should be grounded directly to the ambient since the amount of heat storage in the CNT layer is calculated based on the temperature rise above the ambient temperature. A detailed solution for multilayered structures can be found in [15,16]. As can be seen from Fig. 4, heat generated from the heater diffuses to the ambient through two paths in parallel:

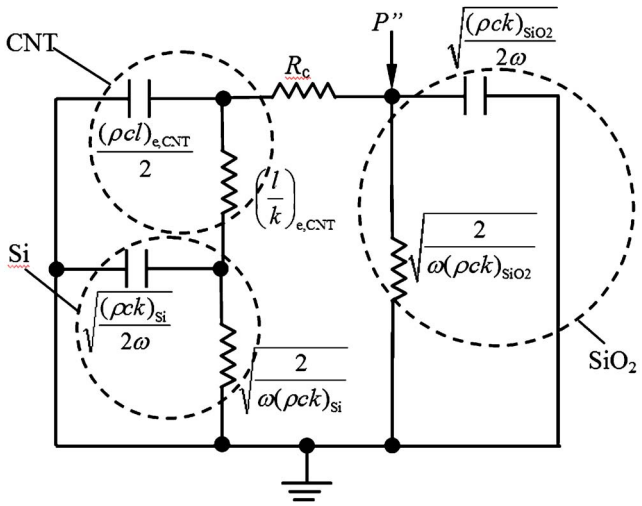

Fig. 4 Equivalent thermal circuit for 1D heat conduction approximation

one through the CNT layer to the silicon substrate and the ambient; the other to the glass substrate and the ambient. The total equivalent thermal impedance $Z_t(\omega)$ can be calculated as

$$\frac{1}{Z_t(\omega)} = \frac{1}{R_C + 1/[(R_{CNT}+Z_{Si}(\omega))^{-1} + j\omega C_{CNT}]} + \frac{1}{Z_{SiO2}(\omega)} \tag{16}$$

The temperature oscillation ΔT then can be predicted as

$$\Delta T = P''\cdot Z_t(\omega) \tag{17}$$

The thermal properties of the CNT sample $k_{e,CNT}$ and $c_{e,CNT}$, as well as the contact thermal resistance R_c are obtained by fitting the temperature oscillation data with the prediction of Eq. (17). The summed square of residues, minimized during the data fitting process, is given by

$$S(k_{e,CNT},c_{e,CNT},R_c(P_1),R_c(P_2)) = \sum_{\omega}[\Delta T_{exp}(\omega) - \Delta T_{mdl}(2\omega)]^2 \tag{18}$$

where $P_1=40$ kPa and $P_2=100$ kPa are attachment pressures, and ΔT_{exp} and ΔT_{mdl} are temperature oscillations obtained from the experiment and modeling, respectively.

It should be noted that the contribution of the CNT layer to the temperature oscillation is different than that of the contact resistance. For variable modulated frequencies, the contact resistance R_c contributes a fixed offset, but the contribution of the CNT layer Z_{CNT} is frequency dependent. For variable attachment pressures, the contact resistance R_c varies with pressure, but, for moderate pressures (such as the pressures of 40 kPa and 100 kPa used herein), the thermal properties of the CNTs should remain the same. Therefore, both the effective thermal properties of the CNT sample and the contact resistance can be subtracted by fitting the experimental data at variable frequencies. Figure 5 shows an example of data fitting at 300 K. The 1D model is clearly sufficient for frequencies higher than 10 Hz. At lower frequencies, heat can diffuse deep into the bulk substrates, and the assumption of 1D heat conduction fails. Therefore, data points at frequencies lower than 10 Hz are excluded from data fitting.

Results and Discussion

Measured results are given in Figs. 6 and 7 for thermal properties and contact thermal resistance, respectively. The hollow points represent measured data and the solid lines shows the slope of temperature dependence. The measurement uncertainty mainly

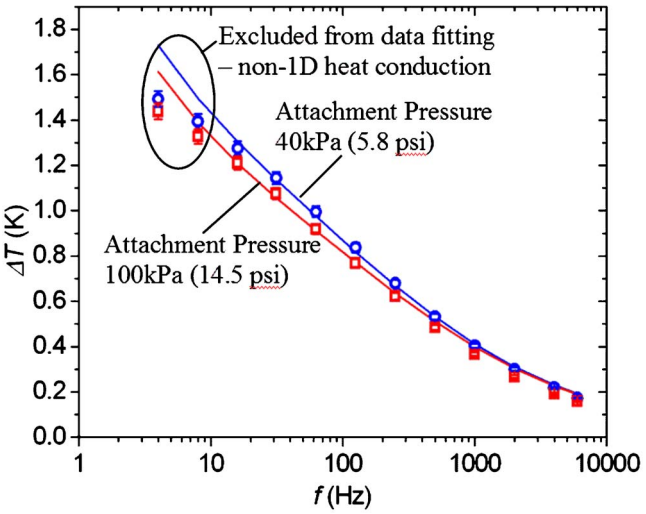

Fig. 5 Observed temperature oscillation amplitudes versus theoretic predictions at 300 K (empty circles and squares are experimental data; solid lines are theoretic predictions)

comes from the uncertainty of the 3-omega signal V_{3w} (about 2%) and the measurements of dT/dR, R_0, and V are found to be very accurate (<0.1%). According to Eq. (1), the uncertainty of the temperature oscillation ΔT_{exp} is also about 2%. The uncertainty of any fitted quantity y ($y=k_{e,CNT}$, $c_{e,CNT}$, $R_c(P_1)$ or $R_c(P_2)$) is then estimated by

$$\left(\frac{\delta y}{y}\right) = \left(\frac{\partial y}{\partial \Delta T}\right)\left(\frac{\delta \Delta T_{exp}}{\Delta T_{exp}}\right) \tag{19}$$

The partial deviation of y with respect to ΔT can be estimated by examining the difference of data fitting after applying an offset of the temperature oscillations. The estimated uncertainties do not include the approximations made to the analytical model.

The measured effective thermal conductivity of the CNT sample is 74 W/m K at 295 K and increases to 83 W/m K at 323 K, an increase of 12%. The specific heat, from the slope of the fitted curve, increases by more than 20% over the same temperature range. Because the thermal conductivity of a CNT is proportional to the product of its volume-based specific heat and its phonon mean free path, the measured results can be explained as follows. At higher temperatures, more phonons occupy higher energy levels and carrying more heat (i.e., higher specific heat), conversely, the phonon mean free path decreases with increasing temperature due to increased phonon-phonon scattering at higher temperatures. The first factor is dominant in the measure temperature range, which increases the thermal conductivity of the CNT sample, but at a smaller percentage than the increase of volume-based specific heat due to the second factor. Another possible reason is the increase of the thermal conductivity of the surrounding air with increasing ambient temperate since the samples are exposed to the air during testing.

The actual thermal conductivity of a CNT itself, considering the volume fraction of the CNT sample, can be hundreds of W/mK. This value is still lower than the theoretical predictions [6] and the measured results for an individual CNT [4]. However, with improvements in CNT quality, the effective thermal conductivity of the aligned CNT layer can potentially increase further. These high thermal conductivity values suggest that the aligned CNT can be a promising candidate for future TIM solutions.

We also note that the contact resistance between the CNT and the heater is rather large, even with increased attachment pressures. This contact resistance includes the resistances summed over the passivation and catalyst layers and the interfaces in between. But this portion should be small because the passivation

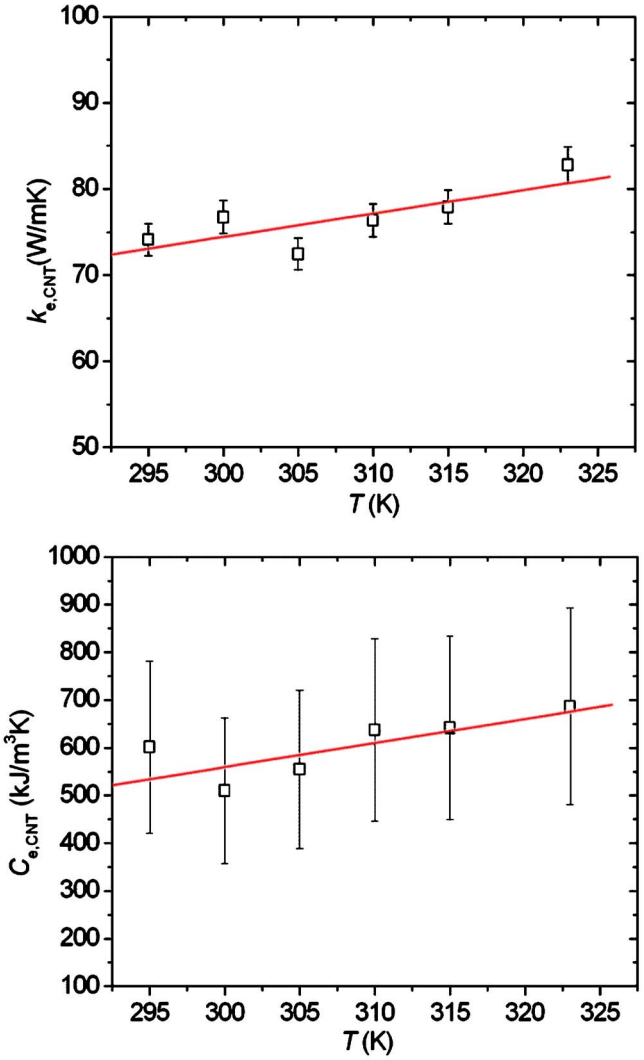

Fig. 6 Measured effective thermal properties (solid lines are linear curve fits)

and catalyst layers are extremely thin and the interfaces are well prepared. The contact resistance is probably dominated by other factors. One problem is that the tubes are not exactly the same length; some of them may not form good mechanical contacts. Better mechanical contacts can be obtained by increasing attachment pressure. However, there exist other fundamental problems that may not be solved with increased pressure, such as constriction effects and acoustic mismatch at the contact points. More experimental and modeling work is needed to understand the fundamental mechanism of the heat transport at the contact points of CNTs.

In practice, a few possible solutions exist to reduce the impact of the contact thermal resistance without an overall increase in attachment pressure. The first method is the combined use of other TIM materials, including thermal greases [9] and phase change materials [17]. The second possible solution is to grow vertically orientated CNTs on both of the contact surfaces to form a CNT cross-talk interface [18].

Conclusions

In summary, vertically oriented CNTs on a silicon substrate have been thermally characterized using a 3ω method. The results indicate that the aligned-CNT layer has much higher thermal conductivity than that of common commercial TIMs, and therefore

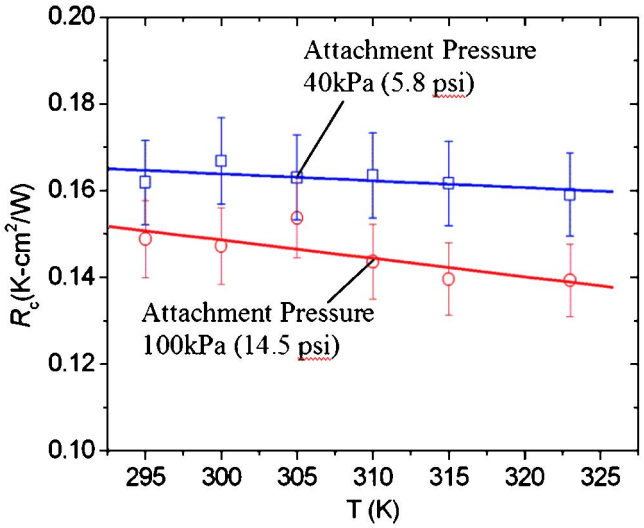

Fig. 7 Measured contact thermal resistance between the CNT sample and the experimental contact (solid lines are linear curve fits)

these materials may be a promising TIM candidate for next-generation electronic packaging. The contact resistance at the tips of the aligned CNTs, however, is still a challenge.

Acknowledgment

This research receives financial support from SRC 2003-NJ-1064 and DARPA N6001-04-1-8916. Purdue authors gratefully acknowledge funding from the Purdue Cooling Technologies Research Center, an NSF I/UCRC.

Nomenclature

a = $\sqrt{j\omega\rho c}/k$, m^{-1}
C = thermal capacitance, J/m^3 K
c = specific heat, J/kg K
f = frequency, Hz
j = imaginary unit
k = thermal conductivity, W/m K
l = thickness, μm
P'' = power density, W/m^2
R = thermal resistance, K m^2/W
R_0 = electrical resistance of the metal bridge, Ω
R_i = electrical resistance of the resistors in the Wheatstone bridge, $i=1,2,3$
S = summed squares of residues, K^2
T = temperature, K
V = electrical voltage along the metal bridge, mV
$V_{3\omega}$ = 3ω voltage component along the metal bridge, mV
$v_{3\omega}$ = Nonequilibrium voltage of the Wheatstone bridge, mV
y = $k_{e,CNT}$, $c_{e,CNT}$, $R_c(P_1)$ or $R_c(P_2)$
Z = thermal impedance, K m^2/W

Greek symbols

ΔT = Temperature oscillation along the metal bridge, K
δ = experimental uncertainty
ϕ = volume fraction
ρ = density, kg/m^3
ω = angular frequency, rad/s

Subscripts

CNT = carbon nanotube
c = contact
e = effective value
exp = experimental measurement
mdl = model prediction
Si = silicon substrate
SiO2 = glass substrate
t = total

References

[1] International Technology Roadmap for Semiconductors, 2003 edition and 2004 update, http://public.itrs.net/
[2] Iijima, S., 1991, "Helical Microtubules of Graphitic Carbon," Nature (London), **354**, pp. 56–58.
[3] Hone, J., Whitney, M., Piskoti, C., and Zettl, A., 1999, "Thermal Conductivity of Single-Walled Nanotubes," Phys. Rev. B, **59**(4), pp. R2514–R2516.
[4] Kim, P., Shi, L., Majumdar, A., and McEuen, P. L., 2001, "Thermal Transport Measurements of Individual Multiwalled Nanotubes," Phys. Rev. Lett., **87**, pp. 215502 (1–4).
[5] Yu, C., Shi, L., Yao, Z., Li, D., and Majumdar, A., 2005, "Thermal Conductance and Thermopower of an Individual Single-Walled Carbon Nanotube," Nano Lett., **5**(9), pp. 1842–1846.
[6] Berber, S., Kwon, Y. K., and Tomanek, D., 2000, "Unusually High Thermal Conductivity of Carbon Nanotubes," Phys. Rev. Lett., **84**(20), pp. 4613–4617.
[7] Choi, S. U. S., Zhang, Z. G., Yu, W., Lockwood, F. E., and Grulke, E. A., 2001, "Anomalous Thermal Conductivity Enhancement in Nanotube Suspensions," Appl. Phys. Lett., **79**(14), pp. 2252–2254.
[8] Biercuk, M. J., Llaguno, M. C., Radosavljevic, M., Hyun, J. K., Johnsond, A. T., and Fischer, J. E., 2002, "Carbon Nanotube Composites for Thermal Management," Appl. Phys. Lett., **80**(15), pp. 2667–2769.
[9] Hu, X., Jiang, L., and Goodson, K. E., 2004, "Thermal Conductance Enhancement of Particle-filled Thermal Interface Materials Using Carbon Nanotube Inclusions," *Proc. 9th Intersociety Conference on Thermal and Thermo-Mechanical Phenomena in Electronic System* (ITHERM), Las Vegas, NV, June 1–4, Vol. 1, pp. 63–69.
[10] Montgometry, S. W., and Holalkere, V. R., 2003, "Carbon Nanotube Thermal Interface Structures," US Patent Application No. 20030117770.
[11] Xu, J., and Fisher, T. S., 2006, "Enhanced Thermal Contact Conductance Using Carbon Nanotube Arrays," IEEE Trans. Compon. Packag. Technol., **29**(2), pp. 261–267.
[12] Cahill, D. G., 1990, "Thermal Conductivity Measurement From 30 to 750 K: The 3ω Method," Rev. Sci. Instrum., **61**(2), pp. 802–808.
[13] Cahill, D. G., Goodson, K. E., and Majumdar, A., 2002, "Thermometry and Thermal Transport in Micro/Nanoscale Solid-State Devices and Structures," J. Heat Transfer, **124**(2), pp. 223–241.
[14] Yamane, T., Nagai, N., Katayama, S., and Todoki, M., 2002, "Measurement of Thermal Conductivity of Silicon Dioxide Thin Films Using a 3ω Method," J. Appl. Phys., **91**(12), pp. 9772–9776.
[15] Touzelbaev, M., 2001, "Thermal Properties of Novel Electronic Materials," Ph.D. dissertation, Stanford Univeristy.
[16] Borca-Tasciuc, T., Kumar, A. R., and Chen, G., 2001, "Data Reduction in 3ω Method for Thin-Film Thermal Conductivity Determination," Rev. Sci. Instrum., **72**(4), pp. 2139–2147.
[17] Xu, J., and Fisher, T. S., 2006, "Enhancement of Thermal Interface Materials With Carbon Nanotube Arrays," Int. J. Heat Mass Transfer, **49**, pp. 1658–1666.
[18] Tong, T., Zhao, Y., Delzeit, L., Kashani, A., and Majumdar, A., 2004, "Multiwalled Carbon Nanotube/Nanofiber Arrays as Conductive and Dry Adhesive Interface Materials," *Proceedings Integrated Nanosystems: Design, Synthesis and Applications Conference*, ASME Conference NANO2004-46013, Pasadena, CA, Sept. 22–24.